Available online at www.sciencedirect.com
SCIENCE DIRECT®
ELSEVIER
International Journal of Solids and Structures 43 (2006) 1543–1560
INTERNATIONAL JOURNAL OF SOLIDS and STRUCTURES
www.elsevier.com/locate/ijsolstr

Some improvements on the energy absorbed in axial plastic collapse of hollow cylinders

A. Abdul-Latif *, R. Baleh, Z. Aboura

L3M, IUT de Tremblay, 93290 Tremblay-en-France, France

Received 23 November 2004; received in revised form 16 April 2005
Available online 13 June 2005

Abstract

The control of the plastic flow mechanism during axial collapse of metallic hollow cylinders is of particular interest in the present work for the absorbed energy. Hence, an experimental methodology is developed during which some different tubular structures are loaded under compressive quasi-static strain rate. These structures of various geometrical parameters $\eta = R_m/t$ and $\lambda = R_m/L$ (R_m: mean radius, L: initial length and t: thickness of tube) are made either from copper or aluminum considered as an energy dissipating system. At this point, the effects of both parameters on the mean collapse load and absorbed energy are appropriately studied. The role of η ratio, which has been largely investigated previously, is studied again. Moreover, it is found that the λ ratio has a non-negligible influence on the deformation mode for a given η. It is well known that the absorbed energy is influenced by the deformation mechanism, i.e., for the axisymmetric mode, the related absorbed energy becomes more important than that of the diamond fold mechanism for a given cylinder. Accordingly, to maximize the absorbed energy, two different structural solutions, namely fixed-ends and subdivided structure, are developed for encouraging the axisymmetric mode. It is convenient to consider the classical axial collapse situation (noted as free-ends) as a comparison reference. In this work, it is recognized that the subdivided solution is relatively the best solution. As a result, the absorbed energy increases up to 21% in comparison with the free-ends situation for copper tubes.

Keywords: Plastic buckling; Energy absorber devices; Collapse modes; Large deformation; Geometrical parameters effects

1. Introduction

The success of the engineering design often depends on an appropriate selection of the specific material with respect principally to its mechanical properties and its reliability, i.e., its safety. One of the most

* Corresponding author. Tel.: +33 1 41 51 12 34; fax: +33 1 48 61 38 17.
E-mail address: aabdul@iu2t.univ-paris8.fr (A. Abdul-Latif).

0020-7683/$ - see front matter © 2005 Elsevier Ltd. All rights reserved.
doi:10.1016/j.ijsolstr.2005.04.029

important engineering application related to mitigating the damage and consequently improving the vehicular crashworthiness, is the energy dissipating systems. A number of literature surveys representing the state of the art in this field, in particular (see, Ezra and Fay, 1970; Rawlings, 1974; Johnson and Reid, 1978, 1986; Jones, 1989; Alghamdi, 2001), give worthy discussions of the design of mechanical devices for dissipating kinetic energy and their related theoretical developments. Bolstered by a host of several developing devices to dissipate the energy, a strong conviction is emerging that the response of structures to a large extent depends on many considerable factors: the effect of large geometry changes, hardening and strain rate effects, and the different modes of deformation governing the interaction between the above factors and the type of the employed material.

The energy absorbed during the plastic deformation is one of the most logical foundations for developing a tool dealing with the energy absorption. Large plastic behavior of mechanical elements (plates, shells, tubes, stiffeners,...) when subjected to various types of load has been the subject of several experimental and theoretical researches over the last decades. Note that these devices, used for this purpose, are usually one-shot items, i.e., once having been plastically deformed, they are discarded and replaced. The main goal of these investigations is to better understand the modes of deformation, then the resulting failure and the energy absorption patterns during collapses. For any given device, the capability to absorb the energy depends, in general, on the magnitude, type and method of application of loads, strain rates, deformation or displacement patterns and material properties (Johnson and Reid, 1978). Moreover, each device has its own characters and features; so to understand the material response during collapse, the plastic flow has to be appropriately determined through experimental procedures.

Since thin-walled cylinders provide practically the widest range of possible uses in these devices, a focusing is thus made here on such elements. They can be plastically flattened due to lateral compression (e.g., DeRutz and Hodge, 1963; Reddy and Reid, 1979; Abdul-Latif, 2000; Nesnas and Abdul-Latif, 2001; Abdul-Latif and Nesnas, 2003; Abdul-Latif, 2004) and can be laterally crushed under local loads (Thomas et al., 1976; Watson et al., 1976, and others). In addition, tubes can be plastically made to turn inside-out or outside-in, known as tube inversion (e.g., Al-Hassani et al., 1972; Al-Qureshi and De Morrais, 1977). These structures can make to split and curl up (for example, Stronge et al., 1983; Atkins, 1987; Lu et al., 1994). Under axial compressive loadings, these elements can also be plastically buckled. Static or dynamic axial crushing of circular and square or rectangular sectioned tubes have been conducted by many research programs and have been reviewed by Abramowicz and Jones (1986), Jones (1989) and Reid (1993).

The axial plastic buckling of tubular elements is the principal framework of the proposed work. It represents a classical problem in solid mechanics, which treat notably the plastic buckling under both static and dynamic conditions. As an energy absorber system, it provides one of the best devices due to, in general, the stability of the average collapse load throughout the entire collapse process and due to the available stroke per unit mass (Johnson et al., 1977). Because of the combination of the bending and stretching deformations and its progression along the tube, hence the buckled tubes ensure that all of the material participates in the absorption of energy by plastic work. It is well known that a tube wall buckles into either an axisymmetric or a diamond fold mechanism. The corresponding post-buckling load has an oscillatory nature. The bibliographical study points out that the η ratio (R/t) is an important key factor, which can determine the deformation mode during axial collapse. In the case where $R/t < 15$ (Johnson and Reid, 1978), the mode axisymmetric becomes predominant for most engineering materials. Nevertheless, the diamond fold mechanism tends to occur for larger values. For a given tube, it is found that the absorbed energy is more important in the mode axisymmetric than that in the diamond mode. It is important to mention here that no analysis has been given which explains why a particular mode shape is adopted by a given tube for a given material.

In this paper, an experimental methodology of axial collapse of cylinders, which represents a well-known issue, is conducted under quasi-static compressive strain rate conditions. The inertia effects during compressive load are totally neglected, since the kinetic energy is totally converted into plastic work. It is found that,

in addition to the η ratio, the λ ratio (R/L) can play an important role especially in controlling the plastic flow mechanism. Few investigations have been carried out to determine the effect of this parameter on the axial collapse of tubes (Andrews et al., 1983; Guillow et al., 2001). In the light of this fact, two different structural solutions are proposed to encourage the axisymmetric mode. Actually, the first tentative is based on the fixation of the tube extremities (fixed-ends situation). The second particular developed solution consists of cutting a given tubular structure in several portions. These portions are coaxially assembled together and separated by non-deformable discs. The effects of the number and the length of portions (i.e., λ ratio) on the flow mechanism are well studied for different η ratios.

2. Choice of the materials

In this study, two metallic materials are investigated. It is a matter of commercial hardened copper (yield tensile stress: 310 MPa) and annealed aluminum alloy (yield tensile stress: 190 MPa) designated according to French standard as NFA51120 and AFNOR A506411 and A50-451 (6060), respectively. It is well known that each material has a good ductility. Their actual chemical compositions, determined by wet chemical analysis, are summarized in Tables 1 and 2.

The used hollow cylindrical specimens have the following dimensions:

For the copper tubes, four internal diameters (d) are chosen: 26, 30, 38 and 52 mm with 1 mm thickness (t), leading respectively to the following radial geometrical ratios (η): 13.5, 15.5, 19.5 and 26.5.

Table 1
Chemical composition of the employed copper

%	Cu	P
Min.	99.9	0.013
Max.		0.05

Table 2
Chemical compositions of the used aluminum

%	Si	Fe	Cu	Mn	Mg	Cr	Zn	Ti	Others	Total	Al
Min.	0.3	0.1		0.35							Rest
Max.	0.6	0.3	0.1	0.1	0.6	0.05	0.15	0.1	0.05	0.15	

Table 3
Chosen lengths of the copper and aluminum tubes with their ratios

	λ Ratio						R_m, mm	η Ratio
	0.66	0.44	0.33	0.22	0.13	0.1		
Copper tubes								
Initial length of the tubes (L), mm	20.4	30.6	40.7	61	101	135	13.5	13.5
	23.5	35.2	47	70.5	119.2	155	15.5	15.5
	29.4	44.1	58.8	88	147	195	19.5	19.5
	40	60	80	120	204	265	26.5	26.5
Aluminum tubes								
Initial length	23.5	35.2	47	70.5	119.2	155	15.5	15.5
	0.6	0.4	0.3	0.2	0.12	0.1		
Initial length	40	60	80	120	200	240	24	12

For the aluminum structures, two distinct sections are also investigated having diameter (d) = 30 and 46 mm and thickness (t) = 1 and 2 mm giving respectively $\eta = 15.5$ and 12. Characterized by the same longitudinal ratio (λ), several initial tube lengths are defined for both metals. Subsequently, they are crushed quasi-statically under compressive loading. It is worth emphasizing that the specimens are not subjected neither to heat treatment nor to special machining operation. The defined lengths of the copper and aluminum cylinders with their ratios are summed up in Table 3.

3. Experimental procedure

All of the employed tubular structures are loaded between the two parallel platens of an Instron Universal Testing Machine (type 1186) under three compressive constant cross head speeds, namely 1, 50 and 500 mm/min at room temperature. Each employed compressive speed gives undoubtedly a quasi-static strain rate. The machine is connected to an acquisition chain to simultaneously record the force and the corresponding displacement during tube crushing operation. In order to ensure the experimental results accuracy, each test is repeated twice under the same experimental conditions (applied speed and temperature). If the differences between the two responses exceed 3%, then another test has to be performed.

3.1. Origin and particularity of the adopted solutions

Based on those results obtained in relevant literature (e.g., Johnson and Reid, 1978; Baleh et al., 2003a,b) as well as on the part of this study, it is noticed that the absorbed energy is evidently influenced by the deformation mode during axial collapse, i.e., the axisymmetric mode is more interesting than the diamond mode from the absorbed energy point of view for a given tubular structure. Since the main goal of this work is to maximize the absorbed energy, two distinguished solutions are therefore developed:

(1) The first one represents a simple idea based on the fixation of the tube extremities (denoted hereafter as fixed-ends situation). As a result, a special rig is designed and manufactured for conducting all the necessary experimental tests (Fig. 1). The rig is made principally up from two hard steel discs (1) fixed

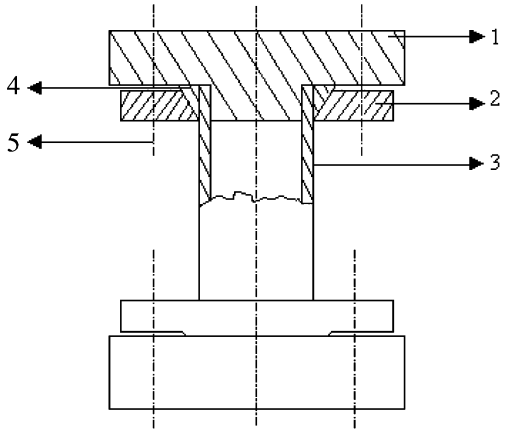

1-hard disc 2-upper clip 3-specimen 4-half-shells 5-tightening screw

Fig. 1. Sectioned view of the assembled rig of the fixed-ends situation tests.

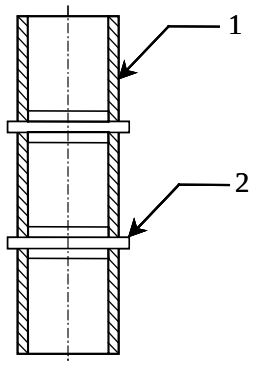

Fig. 2. Sectioned view of the subdivided structure situation tests (3-level arrangement).

over the two machine platens. Two half-shells (4) and a clip (2) over which two conical surfaces are machined and assembled in opposition attached to the discs, maintain the necessary tightening pressure in locking of both structure (3) extremities. It is important to note that only the copper hollow cylinders of 30 mm internal diameter are investigated.

(2) The second developed solution is to cut the initial cylindrical structure in several portions (referred to as subdivided structure). These portions should be assembled together and separated by non-deformable discs made from hard steel (Fig. 2). With a small thickness, the employed discs provide the coaxiality of the superposed tubular portions. This coaxiality is completely guaranteed by an accurate centering between each couple of portions of the tube as shown in Fig. 2. Next, such portions are crushed between the two machine platens.

4. Results and discussion

Once again, the axial collapse of tubes represents one of the most popular energy absorber since it provides an appropriate constant plastic buckling force due to the fact that all of the tube material participates in the absorption of energy by plastic work. Actually, the fundamental question always asked, is how to improve the amount of energy absorbed for given material and structure? This question could be answered, at least partly, by the proposed solution in this work.

Throughout this paper, the notations AM, DM, XM represent respectively, the axisymmetric, diamond fold and mixed modes. For the AM, the classical formed circular undulations represent the zones in which the formation of the plastic localizations (plastic hinges) occurs at the tube perimeter level (Fig. 3a). However, these zones take, in this study, a star form (superposed triangles) in the DM case (Fig. 3b). Furthermore, the symbols F_{av} and F_{max} represent the mean and maximum collapse loads, respectively. Several photos (Figs. 3–5) are also taken to illustrate the plastic buckling progression along the employed tubes, i.e., before, during and after deformation. In order to define the mean collapse load with a maximum of objectivity, especially for those strain hardened materials, it is thus determined using all recorded forces for the whole crushed distance.

Concerning the first remark, it is a matter of the feature of the whole recorded load–deflection curves of the axial buckling of tubes. In fact, these results are in accordance with the experimental observations given in different consulted bibliographic references. The analysis of the experimental results demonstrates the highest peak load, corresponding to initial collapse, followed by a rapid load decrease and then a series of fluctuations about a mean post-buckling load, the peaks and troughs being directly related to

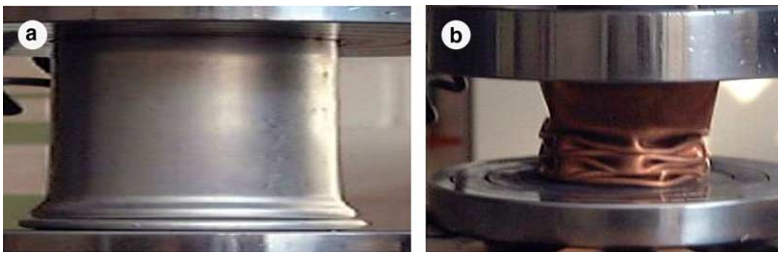

Fig. 3. Plastic buckling of hollow cylinders under free-ends situation: (a) an aluminum specimen showing the beginning of axisymmetric deformation mode and (b) a partially deformed copper specimen with diamond fold mechanism.

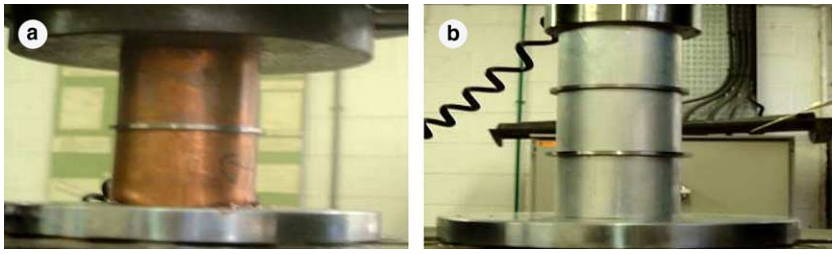

Fig. 4. Two examples of the subdivided structure situation tests using: (a) 2-level (copper cylinders) and (b) 3-level (aluminum specimens).

Fig. 5. Typical example of a fully crushed 3-level subdivided aluminum structure deformed by axisymmetric mode.

the formation of buckles and folding at the various buckling levels (Figs. 7, 9, 12, 15 and 17a). In other words, the tube deforms plastically during which the formation of plastic strain localization zone (plastic hinge) occurs.

4.1. Classical uniaxial crushing of tubular structures

The significant remark, which is taken from the whole experimental results, shows that the λ ratio plays an obvious role on the plastic flow mechanism for the two employed materials. Actually, the obtained results from the copper tests (Table 4) show that greater the value of λ is ($\lambda \geqslant 0.44$), the axisymmetric mode

Table 4
Recorded deformation modes for copper tubes using the free-ends situation

λ	0.66			0.44			0.33			0.22			0.13		
η (for $R_m = \eta$)	13.5	19.5	26.5	13.5	19.5	26.5	13.5	19.5	26.5	13.5	19.5	26.5	13.5	19.5	26.5
L, mm	20.4	29.4	40	30.6	44.2	60	40.7	58.8	80	61	88	120	101	147	200
Cross-head speed, mm/min															
1	AM	AM	AM	AM	AM	AM	AM	AM	DM	AM	DM	DM	DM	DM	DM
50	AM	AM	AM	AM	AM	AM	AM	AM	DM	AM	XM	DM	DM	DM	DM
500	AM	AM	AM	AM	AM	XM	AM	AM	XM	AM	AM	DM	DM	XM	DM

Table 5
Recorded deformation modes for aluminum tubes using the free-ends situation

Deformation mode					
λ (for $R_m = 24$ mm)	0.6	0.4	0.3	0.2	0.12
η (for $R_m = 24$ mm)	12	12	12	12	12
Cross-head speed, mm/min					
1	AM	AM	AM	AM	DM
50	AM	AM	AM	AM	DM
500	AM	AM	AM	DM	DM

becomes predominant whatever the applied loading speed. Hence, in the case where $\lambda = 0.66$ and 0.44, the AM appears in all conducted tests with three distinct η values (13.5, 19.5 and 26.5). However, the DM occurs almost systematically for $\lambda \leqslant 0.13$ whatever the value of η.

Moreover, the same comment is recorded in the case of aluminum tubes as shown in Table 5, but for these values of λ lower or equal to 0.2. Thus, if $\lambda \geqslant 0.2$ (initial tube lengths $\leqslant 80$ mm), the AM almost takes place, otherwise the DM is observed.

It is clear now that the λ ratio (initial tube length) can evidently encourage the axisymmetric mode especially for relatively high values of λ, and gives almost the diamond fold mechanism for lower values at loading speeds ranging from 1 to 500 mm/min.

It is important to underline that the deformation mode transition range depends initially on the value of the η ratio and on the mechanical properties of metals. As a result, the transition phase for the copper tubes having $\eta = 26.5$ is between $\lambda = 0.33$ and 0.44, while it is between 0.2 and 0.3 for the aluminum structures with $\eta = 12$. The obtained results of both metals related to the effect of λ on the collapse mode, for a given η, are in accordance with those results reported in Andrews et al. (1983) and Guillow et al. (2001).

Fig. 6 shows the mean collapse load variation in function of λ under 1 mm/min loading speed. Five tubular structures (three copper tubes and two aluminum ones) are tested showing different load range. In fact, the mean load evolution can be divided in three zones linking up directly to the deformation mode type. The first represents these values corresponding to the DM with $\lambda < 0.22$ for copper and aluminum tubes and $\lambda < 0.2$ for aluminum ones (having $\eta = 12$). Nevertheless, the second phase (transition one) in which the XM appears always. Note that the subsequent mean values increase slightly for all employed structures, due to the increase of the proportion of the AM with respect to the DM in XM, i.e., greater the value of λ is, the AM participation becomes more and more important up to a pure AM for the crushed tube. This corresponds finally the third zone ($\lambda \geqslant 0.44$ for four used structures and $\lambda \geqslant 0.4$ for the aluminum one having $\eta = 12$) in which a maximum crushing mean value can be obtained. Hence, the maximum value of F_{av} for these structures having $\eta = 13.5$, 19.5, 26.5 (copper), 12 and 15.5 (aluminum) are respectively 17, 22, 24, 39 and 11.7 kN. As it has been shown (Andrews et al., 1983; Guillow et al., 2001), it is noteworthy that the values of these two geometrical parameters and notably their interaction determine usually the type of collapse mode for a given material.

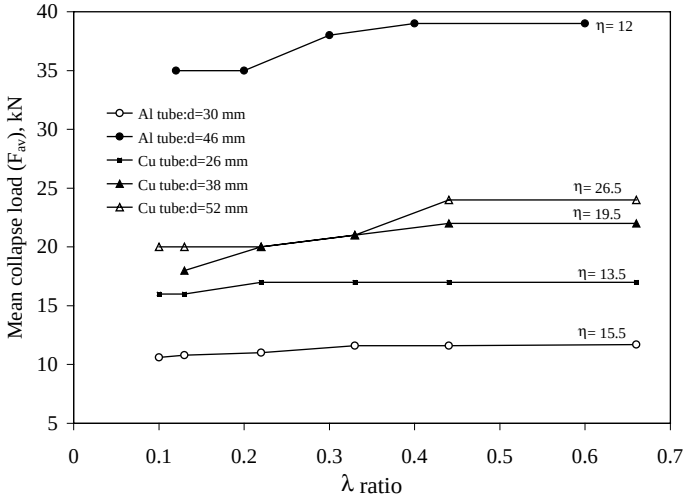

Fig. 6. Effect of the λ ratio on the mean collapse for different copper and aluminum hollow cylinders under free-ends situation at $v = 1$ mm/min.

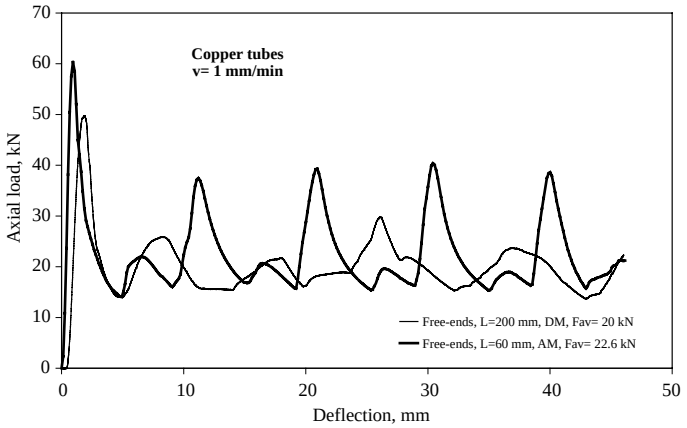

Fig. 7. Evolution of the collapse load versus the axial deflection for the copper tubes with $\eta = 26.5$ under cross-head speed of 1 mm/min using the free-ends situation for two λ ratios of 0.13 and 0.44.

The load–deflection curves for two different copper tubular structures crushed at 1 mm/min loading speed (having $\lambda = 0.13$ and 0.44) are illustrated in Fig. 7. The curve which corresponds the AM for $\lambda = 0.44$, shows clear and regular symmetric peaks with an evolutionary character (oscillatory nature). Alternatively, for $\lambda = 0.13$, the DM is noticeably recorded (Fig. 7). Thus, the evolution of the related curve shows some irregularities. Note also that the peak values in the AM case are undoubtedly higher than those in the DM. Furthermore, the recorded maximum and mean crushing axial loads vary according to the plastic flow mechanism, i.e., they have more important values for the AM than that for the DM. For example, for $\lambda = 0.44$, the obtained values are: $F_{max} = 63$ kN and $F_{av} = 22.6$ kN, whereas for $\lambda = 0.13$, they are: $F_{max} = 49$ kN and $F_{av} = 20$ kN. The difference becomes more perceptible for the maximum loads.

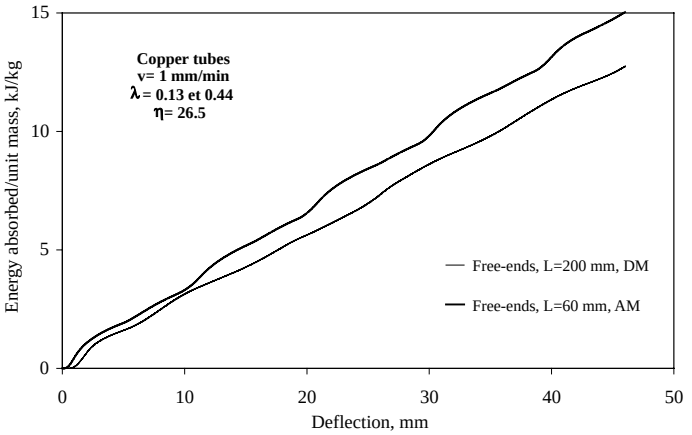

Fig. 8. Evolution of the absorbed energy versus the axial displacement for the copper tubes with $\eta = 26.5$ under $v = 1$ mm/min using the free-ends situation for two λ ratios of 0.13 and 0.44.

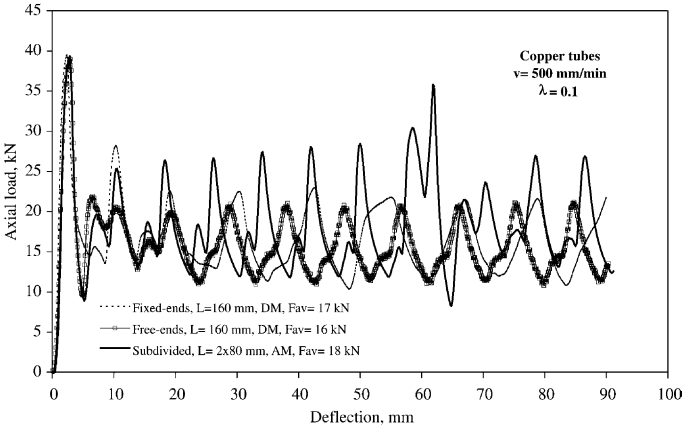

Fig. 9. Load–deflection curves for the copper tubes having $\eta = 15.5$ under loading speed of 500 mm/min for the three structural situations (free-ends, fixed-ends and subdivided structures).

As far as the absorbed energy is concerned, Fig. 8, which describes the absorbed energy variations during tube crushing, points clearly out that the absorbed energy increases up to 10% in the AM case for a particular displacement of 44 mm with respect to DM.

4.2. On the energy absorbed improvement

In order to maximize the energy absorbed during the axial collapse of tubes, the control of the plastic flow mechanism represents a significant key factor as shown above. Therefore, in addition to the classical free-ends case, two different structural situations, fixed-ends and subdivided structure, are currently developed.

Table 6 gives a general comparative summery of the observed results of these three different structural situations for the two metals. In the case where the copper tubes having $\eta = 15.5$ and $\lambda = 0.1$ are axially crushed, it is observed that each situation gives its proper deformation mode. In fixed-ends situation, the

Table 6
Deformation modes and the mean crushing loads for copper and aluminum tubular cylinders in the free-, fixed-ends and subdivided situations

Cross-head speed, mm/min	Copper ($t = 1$ mm)					Aluminum ($t = 2$ mm)			
	$\lambda = 0.1$, $\eta = 15.5$			$\lambda = 0.66$, $\eta = 26.5$		$\lambda = 0.3$, $\eta = 12$		$\lambda = 0.2$, $\eta = 12$	
	Free $L = 160$ mm	Fixed $L = 160$ mm	Subd. $L = 2 \times 80$ mm	Free $L = 120$ mm	Subd. $L = 3 \times 40$ mm	Free $L = 80$ mm	Subd. $L = 2 \times 40$ mm	Free $L = 120$ mm	Subd. $L = 3 \times 40$ mm
1									
F_{av}(Exp.), kN	17	17.7	–	21	24	39	38	38	38
F_{av}(Theo.), kN	17.12[a]	–	–	19.8	24.69	38.8	38.8	38.8	38.8
Def. Mode	XM	DM	–	DM	AM	AM	AM	AM	AM
50									
F_{av}(Exp.), kN	17	17.7	18	20	24	39	38	38	38
F_{av}(Theo.), kN	17[b]	–	18.1	19.8	24.69	38.8	38.8	38.8	38.8
Def. Mode	XM	DM	AM	DM	AM	AM	AM	AM	AM
500									
F_{av}(Exp.), kN	15.9	17.7	18	20	24	39	38	38	38
F_{av}(Theo.), kN	17	–	18.1	19.8	23.8	38.8	38.8	38.3	38.8
Def. Mode	DM	DM	AM	DM	AM	AM	AM	DM	AM

[a] $\alpha = 0.3$ and $\beta = 0.7$.
[b] $\alpha = 0.22$ and $\beta = 0.78$.

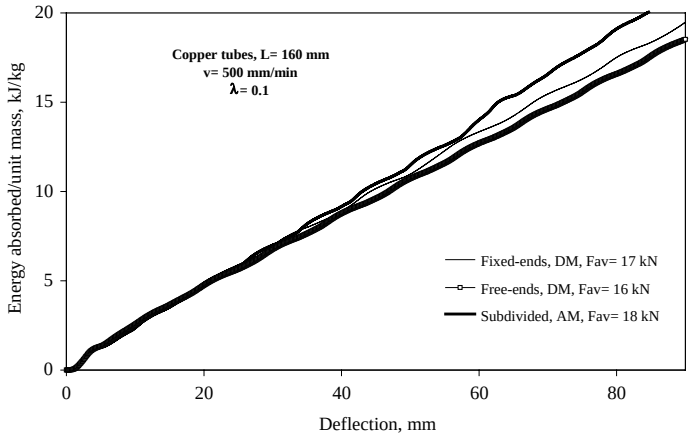

Fig. 10. Evolution of the absorbed energy versus the axial displacement for the copper tubes with $\eta = 15.5$ under cross-head speed of 500 mm/min for the three structural situations.

Fig. 11. Comparative histogram of the energy absorbed using three crushed lengths for the copper tubes having $\eta = 15.5$ under loading speed of 500 mm/min for the free-ends, fixed-ends and subdivided (2-level) structure situations.

dominant mode is, in general, the XM for the free-ends and of DM for $L = 160$ mm, while it is of a AM for the 2-level subdivided structure (2×80 mm) whatever the loading speed. Likewise, the mean crushing load value is globally not affected in the fixed-ends situation; these values increase, however, in the subdivided structure case. Indeed, the latter is responsible for the change in the plastic flow mechanism (AM instead of DM). The same statement can be made concerning the deformation mode for the copper tubes with $\eta = 26.5$ and for the aluminum ones with $\eta = 12$ in free-ends case (with one tube only) and 3-level subdivided structure (3×40 mm). It is worth noting that, for aluminum tubes, the mean crushing load and the corresponding plastic work are not sensitive to the two developed structural situations. This can be interpreted by the fact that the η ratio (for a given λ) plays a more important role than that of the material nature.

As a conclusion, it is found that an increasing in the energy absorption is distinctly recorded in the subdivided structure situation for the copper tubes with $\eta = 15.5$. This is due to the fact that the AM becomes

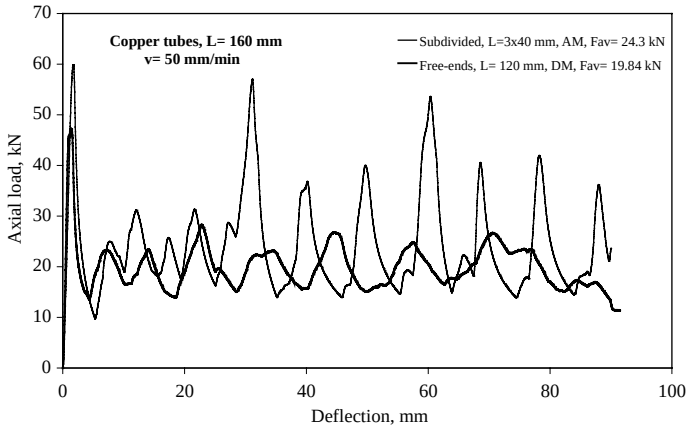

Fig. 12. Load–deflection curves for the copper tubes having $\eta = 26.5$ under loading speed of 50 mm/min for the free-ends (one tube only) and subdivided (3-level) structure situations.

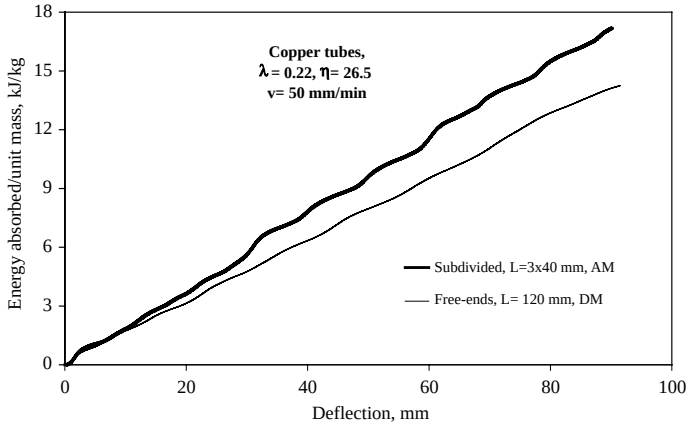

Fig. 13. Evolution of the absorbed enegy versus the axial displacement for the copper tubes having $\eta = 26.5$ at $v = 50$ mm/min for the free-ends (one tube only) and subdivided (3-level) structure situations.

the principal deformation mode whatever the loading speed. The same remark is also obtained in the aluminum tubes (having also $\eta = 15.5$) tested under the same experimental conditions as in copper.

An examination of Fig. 9, which displays the applied load evolution during the axial crushing of copper tubes having $\eta = 15.5$ and $\lambda = 0.1$ at $v = 500$ mm/min using the three adopted solutions, reveals two remarkable upper peaks in the 2-level subdivided solution. Both peaks represent the start of the yielding in the first and then in the second tube portion. The curve of the fixed-ends situation can also be characterized by the first lowest peak elimination in comparison with the other two situations. This seems to be associated with a relative freedom of the plastic flow in the free-ends and subdivided cases and it is not the case in the fixed-ends type. This can explain, despite the DM in the fixed-ends, why a moderate increase in absorbed energy is recorded with respect to the XM in the free-ends case.

The direct apparent result of the deformation mode change in the subdivided structures (AM instead of DM as for the free-ends and fixed-ends structures) is expressed by the increase of the absorbed energy. Hence, Fig. 10 reveals that the subdivided solution provides the best energy absorption capability among

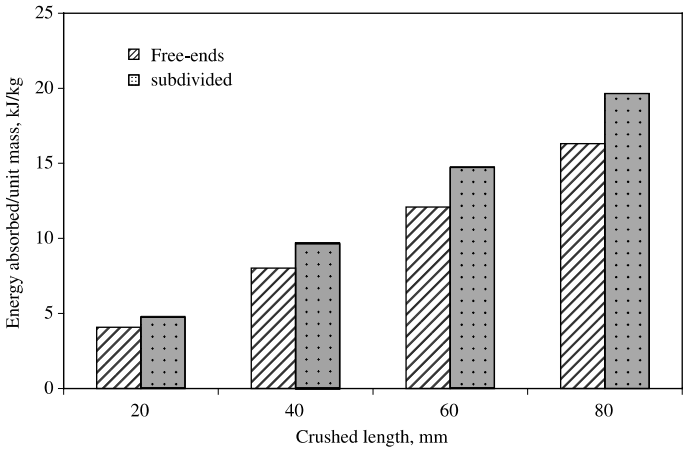

Fig. 14. Comparative histogram of the energy absorbed for four crushed lengths for the copper tubes having $\eta = 26.5$ at $v = 50$ mm/min for the free-ends and subdivided (2-level) structure situations.

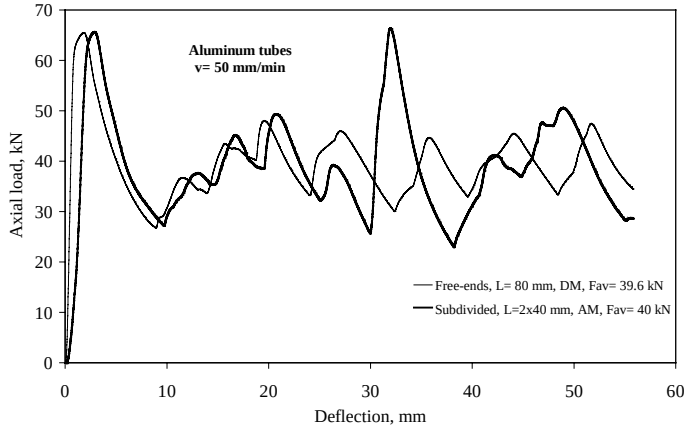

Fig. 15. Load–deflection curves for the aluminum tubes having $\eta = 12$ under $v = 50$ mm/min for a single free-ends and subdivided (2-level) structure situations.

the three. This is confirmed through the increase of the absorbed energy passing thus from 1400 to 1700 J for a given axial deflection of 90 mm. Moreover, in the fixed-ends situation, the same structure consumes a little more energy (1500 J) than that in the free-ends (1400 J). By way of illustration, the histogram in Fig. 11 shows again that the difference among the consumed energies related to three selected axial deflections of 30, 60 and 90 mm becomes distinctly accentuated by passing from the relative small to high axial deflection. The increase in the absorbed energy evolves therefore up to 5% for 30 mm, 10% for 60 mm and 15% for 90 mm for the subdivided structure in comparison with the free-ends structure. While, for the fixed-ends structure, this evolution is almost constant and closed to 5%. The same precedent observation can be also made based on Figs. 12–14 comparing the behavior of a subdivided of three levels with a free-ends situation having $\eta = 26.5$. In fact, Fig. 12 points out the axial crushing load evolution versus the axial deflection. It can easily detect the presence of three relative important peaks concerning the entrance of the three portions in plasticity. For practical applications of energy absorbers (e.g. used in vehicle collision), high force

peaks are not recommended. Therefore, the improvement of the energy absorbers should consider not only the energy absorbing capacity, but also the limit of the force range. In order to minimize these peaks, chamfering of both tube ends is hence necessary. According to a new development preformed by the authors (near future published work), this solution is adopted using the same structures but under dynamic crushing. It is worth intriguing that a change in deformation mode is perceptibly recorded. Actually, the predominant observed plastic flow mechanism is the AM for the three portions, while it is of DM in the free-ends situation using only one tubular structure ($L = 120$ mm), which has an equivalent length to the three portions ($L = 3 \times 40$ mm). It reveals also an increasing of the mean and maximum collapse loads for the subdivided structure, i.e., from $F_{av} = 19.8$ to $F_{av} = 24.3$ kN and from $F_{max} = 47$ to $F_{max} = 60$ kN. Consequently, the absorbed energy becomes more important in the subdivided case than that in the free-ends one (Fig. 13). The difference in energy absorption ability between the two situations can be easily defined by the variation in their slopes. The histogram in Fig. 14 can thoroughly confirm such an observation. In these situations, the variation in absorbed energy becomes more and more significant in favor of the subdivided structure for two selected deflections of 20 and 80 mm passing from 16% to 21%.

As far as the aluminum structure is concerned, contrary to the copper tubes, Figs. 15 and 16 show obviously that there is not a significant effect of the subdivided solution on the plastic work behavior comparing to the free-ends situation whatever λ value (i.e., initial length) and the loading speed. This can be interpreted by the fact that the aluminum tubular structure has relatively a relatively lower value of η (an important thickness) giving thus the AM. This result shows obviously the interplay of these two parameters (η and λ) and its effect in controlling the deformation mode for a given material.

To validate the subdivided solution developed in this study, an other test is carried out using copper tubes of $\eta = 26.5$ with two different initial lengths of 60 and 120 mm leading respectively to λ ratios of 0.44 and 0.22. As demonstrated above, the two tube portions behave differently. In fact, the portion with $\lambda = 0.44$ undergoes the AM, while the second one deforms in its own way, i.e., with the DM type. Fig. 17a displays the load–deflection curves patterns of these tube portions. It is well noticed that a substantial change in the mean collapse load is recorded passing from $F_{av} = 21.5$ kN (for the DM) to 27.5 kN (with AM) as a result of the deformation mode change. It is also recorded that the load amplitude of the AM is practically two times more than that in the DM. Nevertheless, the maximum recorded loads are practically the same for the two portions ($F_{max} = 62$ and 61 kN). Moreover, these results are compared with those results of the copper tubes obtained using the free-ends situation having the same equivalent length

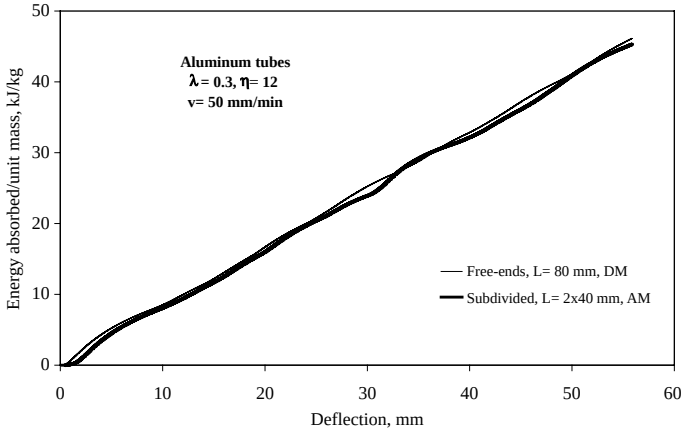

Fig. 16. Evolution of the absorbed energy during the axial collapse of aluminum tubes having $\eta = 12$ at $v = 50$ mm/min for a single free-ends and subdivided (2-level) structure situations.

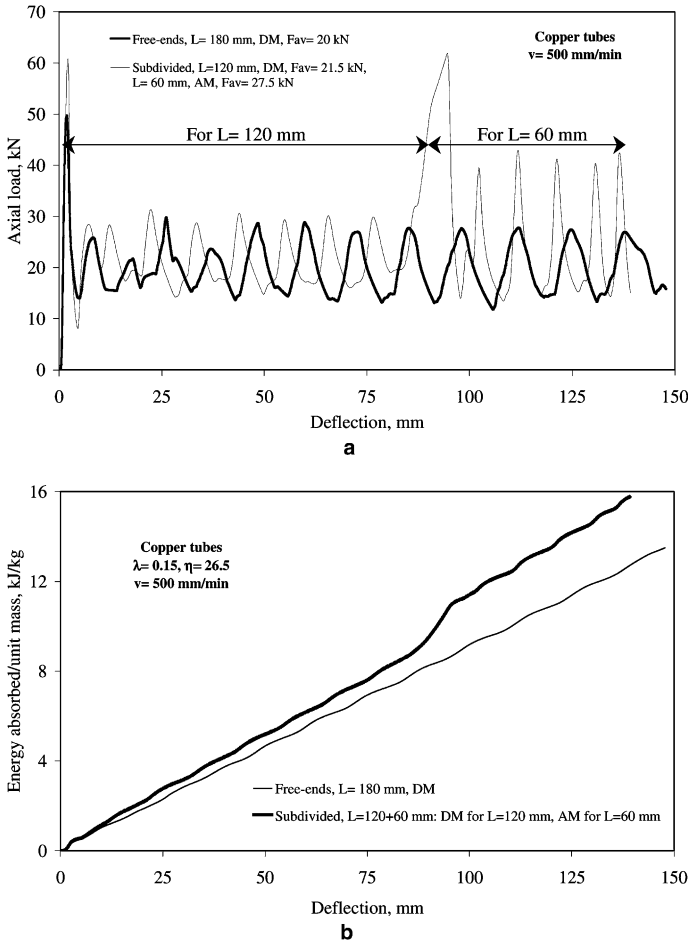

Fig. 17. Influence of the λ ratio on the axial collapse loading fashion (a) and on the absorbed energy (b) in the case of copper tubes having $\eta = 26.5$ at $v = 50$ mm/min for a single free-ends and subdivided structure with two different initial lengths.

($L = 180$ mm). Since the plastic flow mechanism of the latter is DM, thus the corresponding maximum and mean crushing load are respectively $F_{max} = 50$ kN and $F_{av} = 20$ kN (Fig. 17a). Its absorbed energy is demonstrated in Fig. 17b. An evident increase in the absorbed energy takes place once the deformation mode changes from DM to AM. This can be conveyed by increasing the slope of an almost linear absorbed energy–displacement relationship. Whereas, in the free-ends situation, the obtained result is of a monotone trend, i.e., having a classical evolution increasing proportionally and linearly with axial displacement.

5. Theoretical considerations of the axial plastic collapse of hollow cylinders

The classical analytical approaches of Alexander (1960) and Pugsley and Macaulay (1960) proposed to model the axial plastic buckling of circular uniform tubes are employed. Considering the axisymmetric mode, Alexander's model assumes that no interaction between the bending and hoop stresses and the material has a rigid-plastic behavior. However, Pugsley and Macaulay's model represents a semi-empirical

theoretical to estimate the mean load of the diamond fold mechanism based especially on the geometrical argument.

In this study, these models are used to determine the mean collapse load for the copper and aluminum hollow cylinders. A small modification is proposed to take into account the work hardening in both deformation modes.

Classically, Alexander proposes the following mathematical relation to evaluate the mean load:

$$F_{\text{av-A}} = K_{\text{A}} t \sigma_{\text{y}} \sqrt{td}, \tag{1}$$

where, d and t are respectively the mean radius and thickness of tube in mm, σ_{y} is yield tensile stress and K_{A} is approximately equal to 6.

As far as the plastic flow mechanism of a diamond fold type is concerned, the model of Pugsley and Macaulay defines the mean load by

$$F_{\text{av-D}} = \sigma_{\text{y}} \pi t (d - t) \left[K_{\text{D}} \left(\frac{t}{d} \right) + 0.12 \right]. \tag{2}$$

In this approach, K_{D} is a material parameter. According to Mamalis and Johnson (1983), it is equal, for example, to 10 for steel.

The simple modification of the Alexander's model is proposed by adding a new parameter (K_{N}). This parameter, being considered as a correction term, can globalize the hardening effect and the interaction between the bending and hoop stresses on the mean collapse load. Thus, the modified Alexander's equation can be deduced as

$$F_{\text{av-A}} = K_{\text{A}} K_{\text{N}} t \sigma_{\text{y}} \sqrt{td}. \tag{3}$$

In the framework of the third configuration (mixed mode), it is assumed that this mode can be mathematically estimated by combining the Eqs. (2) and (3) and multiplying each part by its related length fraction. Therefore, the mean collapse load of this deformation mode can be written as

$$F_{\text{av}} = \alpha F_{\text{av-A}} + \beta F_{\text{av-D}}, \tag{4}$$

where, α and β are the related length fraction of the axisymmetric and diamond modes, respectively.

In order to determine the mean load whatever the deformation mode, the above equations are used. Hence, the new parameters K_{N} and K_{D} have to be first identified for both employed metals. The yield stresses σ_{y} for the aluminum and copper are respectively 310 MPa and 190 MPa. The overall closeness between the experimental and theoretical results which provide a good general fit give us: $K_{\text{N}} = 1.78$ (for both metals) and $K_{\text{D}} = 14.5$ and 14 for the aluminum and copper tubes, respectively. The comparison between the experimental and theoretical results is summed up in Table 6. It is obviously remarked that the correlated solutions reproduce successfully the experimental results. To validate such calibrated parameters, the mean collapse loads for two aluminum tubes are simulated having the same section ($\eta = 15.5$) and two different initial lengths leading to $\lambda = 0.33$ and 0.13 (giving respectively, MA and DM). Note that the experimental results of these aluminum tubes are not used in the calibration of K_{N} and K_{D}. The correlated result for the DM case is $F_{\text{av}} = 10.32$ kN and its corresponding experimental results is 10.7 kN. On the other hand, for the AM, the predicted and experimental mean loads are equal to 11.1 kN and 11.6 kN, respectively. These results confirm the success of this simple modified approach in describing the experimental observation.

6. Remarks and conclusions

Motivated by its sensitivity to some geometrical parameters, the plastic flow mechanism of the axial collapse of hollow cylinders of different geometries (initial lengths and sections) are investigated under

compressive quasi-static strain rates. Therefore, an experimental study is conducted on copper and aluminum structures of different geometrical ratios $\eta = R_m/t$ and $\lambda = R_m/L$. It is well known that the effect of η ratio on the deformation mode has been well studied previously. Moreover, the λ ratio has an obvious influence on the deformation mode for a given η. These parameters play an important role not only on the mean collapse load and absorbed energy but also on the deformation mode. It is clear now that the λ ratio (i.e., initial tube length for a given section) can evidently encourage the AM especially for relatively high values of λ; and for lower values, it gives almost the diamond fold mechanism at loading speeds ranging from 1 to 500 mm/min. It is important to mention that despite the important role of the parameter λ (for a given η ratio), investigations for other extreme configurations related notably to η are therefore necessary for relatively small wall thickness.

As it is well known that with the AM, the tube absorbs more energy than that with the DM for a given tube, hence the proposed improvements concerning the absorbed energy is based on the control of plastic flow mechanism. Consequently, two new structural solutions (fixed-ends and subdivided structures) are developed to encourage the AM. In the subdivided case, the direct result of the change in deformation mode (AM instead of DM) is expressed by increasing the absorbed energy. Thus, it can be concluded that the subdivided structure provides relatively the best energy absorption capability. This is quantitatively confirmed via an increasing of the absorbed energy in the order of 300 J for copper tubes (i.e., passing from 1400 to 1700 J for an axial deflection of 90 mm).

The proposed simple theoretical modification can successfully describe the axial plastic collapse of hollow cylinders with different geometrical ratios for the used metals.

References

Abdul-Latif, A., 2000. On the lateral collapse of an identical pair of cylinders. Int. J. Solids Struct. 37, 1955–1973.

Abdul-Latif, A., 2004. Using the superplastic as a representative material to simulate the behavior of rate sensitive engineering materials at high strain rates, EURO-SPF 2004, July 7–9, Ecole des Mines d'Albi-Carmaux.

Abdul-Latif, A., Nesnas, K., 2003. Plastic collapse of cylinders under constrained sides and length conditions. J. Eng. Mater. Technol. ASME 125, 215–221.

Abramowicz, W., Jones, N., 1986. Dynamic progressive buckling of circular and square tubes. Int. J. Impact Eng. 4, 243–270.

Alexander, J.M., 1960. An approximate analysis of the collapse of thin cylindrical shells under axial loading. Quart. J. Mech. Appl. Math. 13, 11–16.

Alghamdi, A.A.A., 2001. Collapsible impact energy absorbers: An overview. Thin Wall. Struct. 39, 189–213.

Al-Hassani, S.T.S., Johnson, W., Lowe, W.T., 1972. Characteristics of inversion tubes under axial loading. J. Mech. Eng. Sci. 14, 370–381.

Al-Qureshi, H.A., De Morrais, G.A., 1977. Analysis of multi-version of tube ends. Design Eng. Conf. ASME paper No. 77-DE-35.

Andrews, K.R.F., England, G.L., Ghani, E., 1983. Classification of axial collapse of cylinder tubes under quasi-static loading. Int. J. Mech. Sci. 25, 687–696.

Atkins, A.G., 1987. On the number of cracks in the axial splitting of the ductile metal tubes. J. Mech. Eng. Sci. 29, 115–121.

Baleh, R., Abdul-Latif, A., Aboura, Z., 2003a. Grande déformation de structures tubulaires: systèmes d'absorption d'énergie. CNRIUT 2003, 15–16 mai 2003, (Tarbes).

Baleh, R., Abdul-Latif, A., Aboura, Z., 2003b. Etude Expérimentale sur un Système d'Absorption d'Energie par Ecrasement Axial, 16ème Congres Français de Mécanique, 1–5 September, Nice.

DeRutz, J.A., Hodge, J.R., 1963. Crushing of a tube between rigid plates. J. Appl. Mech. 30, 391–395.

Ezra, A.A., Fay, R.J., 1970. An assessment of energy absorbing devices for prospective use in aircraft impact situation. In: Hermann, G., Perrone, N. (Eds.), Dynamic Response of Structures. Pergamon Press.

Guillow, S.R., Lu, G., Grzebieta, R.H., 2001. Quasi-static compression of thin-walled circular aluminum tubes. Int. J. Mech. Sci. 43, 2103–2123.

Johnson, W., Reid, S.R., 1978. Metallic energy dissipating systems. Appl. Mech. Rev. 31, 277–288.

Johnson, W., Reid, S.R., 1986. Metallic energy dissipating systems. Rev. 31, 277–288. Appl. Mech. Update 1986, pp. 315–319.

Johnson, W., Soden, P.D., Al-Hassani, S.T.S., 1977. In extensional collapse of thin-walled tubes under axial compression. J. Strain Anal. 12, 317.

Jones, N., 1989. Structural Impact. Cambridge Press, Cambridge, UK.
Lu, G., Ong, L.S., Wang, B., Ng, H.W., 1994. An experimental study on tearing energy in splitting square metal tubes. J. Mech. Eng. Sci. 36, 1087–1097.
Mamalis, A.G., Johnson, W., 1983. The Quasi-static crumpling of thin-walled circular cylinders and frusta under axial compression. J. Mech. Eng. Sci. 25, 713–732.
Nesnas, K., Abdul-Latif, A., 2001. Lateral plastic collapse of cylinders: Experiments and modeling. Comput. Model. Eng. Sci. 2, 373–388.
Pugsley, A.G., Macaulay, M., 1960. The large scale crumpling of thin cylindrical columns. Quart. J. Mech. Appl. Math. 13, 1–9.
Rawlings, B., 1974. Response of structures to dynamic loads. In: Proc. Conf. on Mechanical Properties of Materials at High Rates of Strain. Institute of Physics Conference, pp. 279–298.
Reddy, T.Y., Reid, S.R., 1979. Lateral compression of tubes and tube-systems with side constraints. Int. J. Mech. Sci. 21, 187–199.
Reid, S.R., 1993. Plastic deformation mechanisms in axially compressed metal tubes used as impact energy absorbers. Int. J. Mech. Sci. 35, 1035–1052.
Stronge, W.J., Yu, T.X., Johnson, W., 1983. Long stroke energy dissipation in splitting tubes. J. Mech. Eng. Sci. 25, 637.
Thomas, S.G., Reid, S.R., Johnson, W., 1976. Large deformations of thin-walled circular tubes under transverse loading-I. Int. J. Mech. Sci. 18, 325–333.
Watson, A.R., Reid, S.R., Johnson, W., Thomas, S.G., 1976. Large deformations of thin-walled circular tubes under transverse loading-II. Int. J. Mech. Sci. 18, 387–397.